

On dipole compression modes in nuclei

G. Colò^{a*}, N. Van Giai^b, P.F. Bortignon^a and M.R. Quaglia^c

November 2, 2018

^a Dipartimento di Fisica, Università degli Studi, and INFN, Via Celoria 16, I-20133 Milano (Italy)

^b Institut de Physique Nucléaire, IN2P3-CNRS, F-91406 Orsay (France)

^c Dipartimento di Fisica Teorica, Università degli Studi, and INFN, via P. Giuria 1, I-10125 Torino (Italy)

Abstract

Isoscalar dipole strength distributions in spherical medium- and heavy-mass nuclei are calculated within random phase approximation (RPA) or quasiparticle RPA. Different Skyrme-type interactions corresponding to incompressibilities in the range 200 - 250 MeV are used. The results are discussed in comparison with existing data on isoscalar giant dipole resonances. Two main issues are raised, firstly the calculated giant resonance energies are somewhat higher than the observed ones, and secondly a sizable fraction of strength is predicted below 20 MeV which needs to be experimentally confirmed.

PACS: 24.30.Cz, 21.60.Jz

Keywords: giant resonances, nuclear incompressibility, HF-RPA, quasiparticle RPA.

*Tel.: + 39 - 02 - 2392261; fax: + 39 - 02 - 2392487; e-mail: colo@mi.infn.it

The isoscalar giant dipole resonance (ISGDR) is a compressional mode, like the well known isoscalar giant monopole resonance (ISGMR), and its energy is related to the nuclear incompressibility K_∞ [1]. For this reason it has been studied both experimentally and theoretically for many years, as reviewed in [2]. It can be associated with the operator

$$\hat{D} = \sum_{i=1}^A r_i^3 Y_{1\mu}(\hat{r}_i) \quad (1)$$

and it can be viewed as a non-isotropic compression mode.

Although some first indications about the energy location of this mode date back to the beginning of the eighties, more recent evidence of the ISGDR in ^{208}Pb has been reported [3] from the 0^0 measurements of 200 MeV inelastic α -scattering at the Indiana University cyclotron facility. Further evidence based on extensive angular distributions at near- 0^0 angles has since come from 240 MeV inelastic α -scattering experiments at Texas A&M University. The ISGDR strength has been extracted in a large number of nuclei using a multipole decomposition of the observed inelastic scattering spectra. The results for medium- and heavy-mass nuclei like ^{90}Zr , ^{116}Sn , ^{144}Sm and ^{208}Pb are reported in [4]. The measured strength is spread over a wide energy range between 15 and 30 MeV and it is claimed to exhaust nearly 100% of the appropriate energy-weighted sum rule (EWSR). The values of the centroid energy $E_0 \equiv m_1/m_0$ are 26.3(4), 24.3(3), 23.0(3) and 20.3(2) MeV respectively in the four nuclei quoted above (the moments m_k of the strength distribution are defined as $m_k \equiv \sum_n | \langle n | \hat{D} | 0 \rangle |^2 (E_n - E_0)^k$).

Here, we report the ISGDR results calculated with effective Skyrme interactions, within self-consistent Hartree-Fock (HF) plus Random Phase Approximation (RPA) in the case of ^{208}Pb , and Hartree-Fock-BCS (HF-BCS) plus quasi-particle RPA (QRPA) for the other, non double-magic nuclei. The Skyrme forces used in this work are: SkP [5], SGII [6], SKM* [7], SLy4 [8] and SkI2 [9]. They span a range of values of K_∞ from 200 to 250 MeV. The HF mean field is first calculated in coordinate space, then the single-particle spectrum of occupied and unoccupied states is built by diagonalizing the mean field on a harmonic oscillator basis. Details of RPA calculations can be found in Ref. [10]. The dimension of the 1particle-1hole (1p-1h) space is fixed by requiring the exhaustion of the RPA m_1 sum rule. In the HF-BCS calculations constant pairing gaps Δ are introduced according to the usual

12 MeV/ \sqrt{A} parametrization. The QRPA matrix equations are solved with a procedure which parallels what has been said for RPA, with the two quasi-particle configurations replacing the 1p-1h ones. The method is the same as that of Ref. [11].

In the ISGDR problem, one has to face the question of the spurious state associated with the center-of-mass motion which carries the same quantum numbers $J^\pi = 1^-$. In a bona fide self-consistent RPA the spurious state would appear as an eigenstate at zero energy, exhausting the whole strength of the operator

$$\hat{S} = \sum_{i=1}^A r_i Y_{1\mu}(\hat{r}_i) \quad (2)$$

and orthogonal to all other physical states. However, in actual calculations the spurious state is at low but not zero energy because of small numerical inaccuracies and therefore, strength associated with the operator \hat{S} will be shared among the physical states. Starting from the actual RPA set of states $|n'\rangle$, we construct a new set of normalized states $|n\rangle$,

$$|n\rangle = \mathcal{N}_n(|n'\rangle - \alpha_n |S\rangle), \quad (3)$$

where the state $|S\rangle$ is defined as

$$|S\rangle \equiv \hat{S}|0\rangle, \quad (4)$$

$|0\rangle$ being the RPA vacuum. According to [12] we associate to $|S\rangle$ the transition density

$$\alpha_S \frac{d\rho_0}{dr} \quad (5)$$

where ρ_0 is the HF ground state density. The state $|n\rangle$ is required to satisfy the condition $\langle n|\hat{S}|0\rangle = 0$, i.e.,

$$\int dr r^3 (\delta\rho_{n'} - a_n \frac{d\rho_0}{dr}) = 0, \quad (6)$$

where $\delta\rho_{n'}$ is the transition density of the RPA state $|n'\rangle$ defined in the usual way. The problem of the spurious state normalization α_S is circumvented by the use of Eq. (6) since $a_n \equiv \alpha_n \alpha_S$ is well behaved (i.e., not divergent).

The difference between the strength distributions associated with the states $|n'\rangle$ and $|n\rangle$ is shown in the top-left corner of Fig. 1, for the typical case of ^{208}Pb with the force SGII. The strengths are essentially the same

in the energy range which will be denoted “giant resonance (GR) region” (this range is evident from the plot but it is explicitly indicated in Tables 1 and 2). At lower energies, omitting the projection procedure can lead to a serious overestimation of the ISGDR strength. It is clear nevertheless from Fig. 1 that a non-negligible amount of non-spurious strength is present in the energy range which will be called “low-energy region”. This low-lying strength is due to $1 \hbar\omega$ excitations, which of course can contain strength associated with the \hat{D} operator.

Another way of eliminating the spurious strength is to keep the $|n'\rangle$ states and to replace the operator (1) by

$$\hat{D}_{modif} = \sum_{i=1}^A (r_i^3 - \eta r_i) Y_{1\mu}(\hat{r}_i), \quad (7)$$

where $\eta = \frac{5}{3}\langle r^2 \rangle$. This prescription was derived and used in Ref. [13]. Although the derivation is based on hydrodynamical-type arguments, one thus obtains strength distributions which are almost indistinguishable to those calculated with the present projection procedure. One may also note that in Ref. [14] a different prescription was used for the subtraction of spurious strength resulting in an almost disappearance of strength in the low-energy region.

In Fig. 1 we also show center-of-mass corrected strength distributions for the other nuclei calculated with a typical interaction, namely SGII. The general features are: a) a large fraction of the strength lies in the GR region, and b) a non negligible amount of strength is in the low-energy region. The latter region contains about 20% of the ISGDR energy-weighted sum rule. These features are common to the results obtained with the other interactions. A more detailed analysis in terms of the moments m_0 and m_1 is reported in Table 1 for ^{208}Pb and all interactions, and in Table 2 for all 4 nuclei and the SGII interaction.

In comparison with the existing data, there are two main issues to be faced. First, there is a large discrepancy between predicted and measured GR energies, much larger than in all other GR cases. This is the more puzzling that the same model employed here was used successfully to describe the ISGMR in ^{208}Pb [15]. Second, the calculations predict a sizeable amount of strength at low-energy, which needs to be experimentally confirmed [16]. These features are common to the calculated strength distributions of the

operator $j_1(qr)Y_{1\mu}(\hat{r})$, which is a generalization of Eq.(1). In particular, they remain peaked at the same energies as the strength distribution of \hat{D} for values of q up to 0.6 fm^{-1} .

In Fig. 2 we show the predicted peak and centroid energies of the GR region for various nuclei as a function of K_∞ . The experimental values of E_0 for the GR region quoted above [4] would be outside the figure, except for ^{90}Zr . The discrepancy appears very severe in Pb and Sn. In what follows we concentrate on Pb because it is the nucleus where the HF+RPA model should work better.

Earlier RPA calculations [17] performed with the finite range Gogny interaction already found that the ISGDR energy was in the range of 26 MeV, in qualitative agreement with the present results and with Ref. [13]. One might expect that effects beyond RPA, like the coupling to 2p-2h excitations would somewhat lower the centroid energy. However, the calculations of Ref. [18] find a downward shift of less than 1 MeV. The ISGDR has also been calculated in the relativistic RPA approach [19] in ^{208}Pb and ^{144}Sm and it is found that, for effective lagrangian parametrizations corresponding to K_∞ in the range 200-270 MeV the energy of the ISGDR is of the order of 25 MeV. Thus, the question of understanding the observed values of E_0 is still open.

As for the low-energy region, our analysis of the configurations involved for instance in ^{208}Pb , shows that the strength comes from bound-to-bound neutron transitions like $h_{9/2} \rightarrow i_{11/2}$, $i_{13/2} \rightarrow j_{15/2}$ and, in some cases, $f_{5/2} \rightarrow g_{7/2}$. In the data reported in Ref. [4] no low-lying strength is present. Further analysis of the same data is currently in progress [16], which may reveal the presence of isoscalar strength around the region of the isovector dipole.

In conclusion, we report in this paper HF+RPA and HF-BCS+QRPA calculations of the ISGDR in ^{90}Zr , ^{112}Sn , ^{144}Sm and ^{208}Pb nuclei. Two general features appear from the calculated strength distributions: some large resonance-type distribution of strength in the $110A^{-1/3} \text{ MeV}$ energy region and some smaller, but still sizeable fraction of the strength below 20 MeV. These two characteristic features do not seem to agree quantitatively with the observation.

We thank D.H. Youngblood for helpful discussions about the experimental data analysis, and U. Garg for discussions. P.F.B. thanks IPN-Orsay for the warm hospitality during the time when this work was completed.

References

- [1] S. Stringari, Phys. Lett. **B108** (1982) 232.
- [2] U. Garg, RIKEN Review **23** (1999) 65.
- [3] B.F. Davies et al., Phys. Rev. Lett. **79** (1997) 609.
- [4] H. Clark et al., Nucl. Phys. **A649** (1999) 57c.
- [5] J. Dobaczewski, H. Flocard and J. Treiner, Nucl. Phys. **A422** (1984) 103.
- [6] Nguyen Van Giai and H. Sagawa, Phys. Lett. **B106** (1981) 379.
- [7] J. Bartel, P. Quentin, M. Brack, C. Guet and H.B. Håkansson, Nucl. Phys. **A386** (1982) 79.
- [8] E. Chabanat, P. Bonche, P. Haensel, J. Meyer, R. Schaeffer, Nucl. Phys. **A635** (1998) 231.
- [9] P.-G. Reinhard and H. Flocard, Nucl. Phys. **A584** (1995) 467.
- [10] G. Colò, Nguyen Van Giai, P.F. Bortignon and R.A. Broglia, Phys. Rev. **C50** (1994) 1496.
- [11] E. Khan and N. Van Giai, Phys. Lett. **B472** (2000) 253.
- [12] G.F. Bertsch, Suppl. Progr. Theor. Phys. **74** (1983) 115; E. Lipparini and S. Stringari, Phys. Rep. **175** (1989) 103.
- [13] N. Van Giai and H. Sagawa, Nucl. Phys. **A371** (1981) 1.
- [14] I. Hamamoto, H. Sagawa and X. Zhang, Phys. Rev. **C57** (1998) R1064.
- [15] G. Colò, P.F. Bortignon, Nguyen Van Giai, A. Bracco and R.A. Broglia, Phys. Lett. **B276** (1992) 279.
- [16] D.H. Youngblood, private communication.
- [17] J. Dechargé and L. Šips, Nucl. Phys. **A407** (1983) 1.
- [18] G. Colò, Nguyen Van Giai, P.F. Bortignon and M.R. Quaglia, RIKEN Review **23** (1999) 39.

[19] Z.Y. Ma and N. Van Giai, preprint nucl-th/9910054.

Fig. 1. ISGDR strength distributions calculated with the interaction SGII and corrected for center-of-mass effects. In the case of ^{208}Pb the dashed line corresponds to a calculation without proper subtraction of the spurious center-of-mass state (see text).

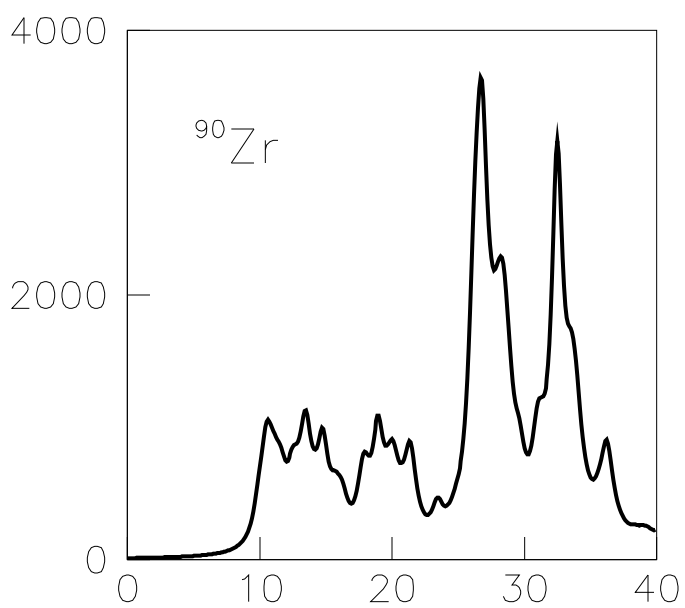
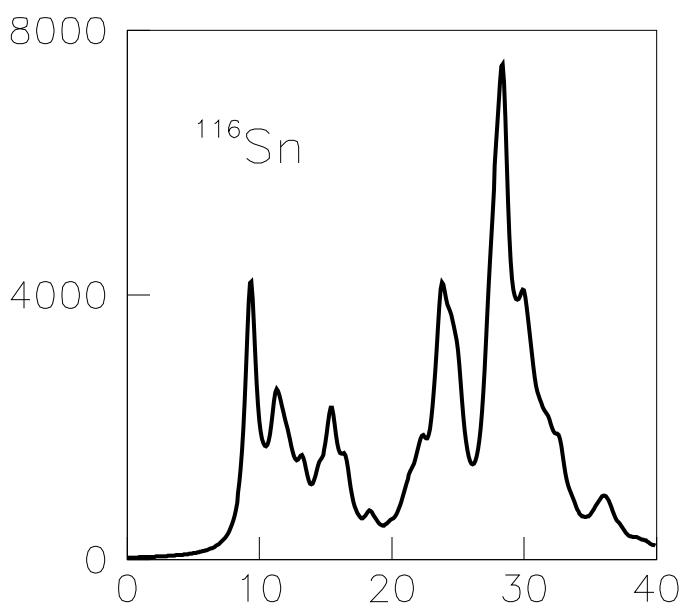
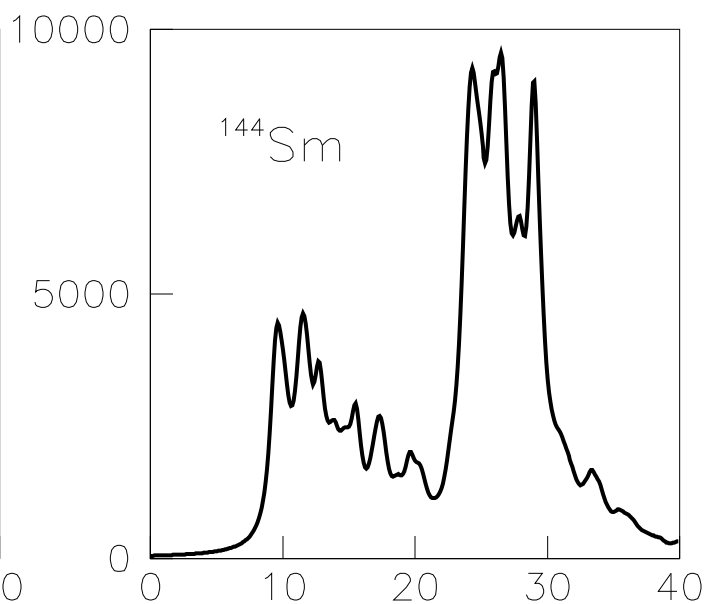
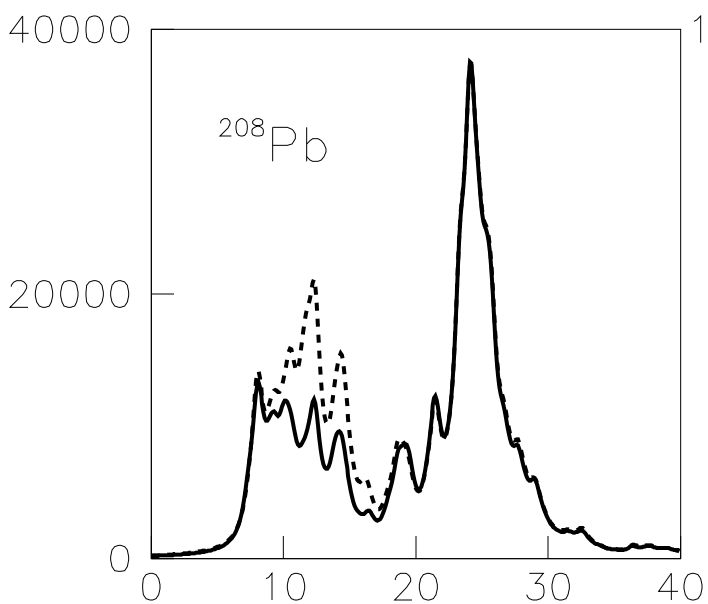
Fig. 2. Centroid energies E_0 (black circles) and peak energies (open circles) of the GR regions, determined by using different Skyrme interactions and plotted as a function of K_∞ . The full and dashed lines are drawn as a guide to the eye.

Table 1: Integral properties of the ISGDR strength distribution in ^{208}Pb calculated with different forces. The corresponding incompressibilities are indicated in MeV. Results for the low-energy region (0-17 MeV) and the GR region (17-30 MeV) are separated. For each region the values of m_0 and m_1 are given in units 10^5fm^6 and $10^6\text{fm}^6\cdot\text{MeV}$, respectively. The last column shows (in MeV) the centroid energies m_1/m_0 of the GR region, and the peak energies in parenthesis.

Force	K_∞	Low-energy region		GR region		
		m_0	m_1	m_0	m_1	m_1/m_0
SkP	201	0.85	0.89	1.86	4.25	22.8 (23.6)
SGII	215	0.90	0.98	1.61	3.85	23.9 (24.1)
SkM*	217	0.94	1.01	1.67	3.96	23.7 (24.2)
SLy4	230	0.92	0.99	1.51	3.67	24.3 (25.2)
SkI2	241	1.02	1.05	1.58	3.88	24.6 (25.3)

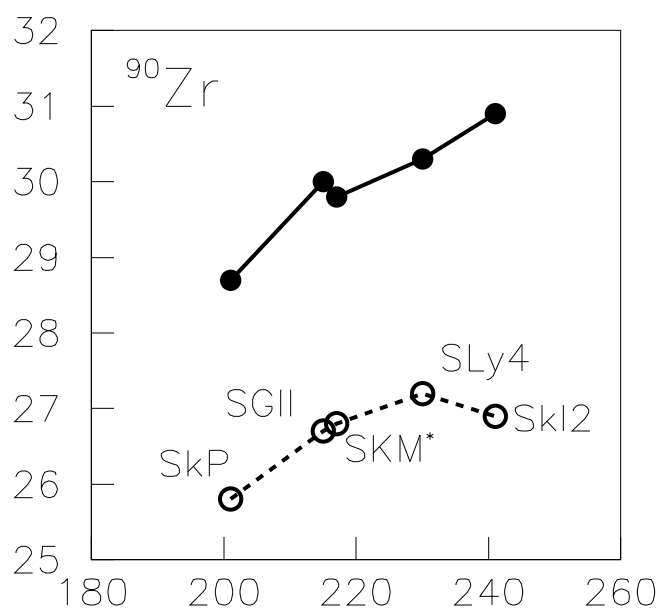
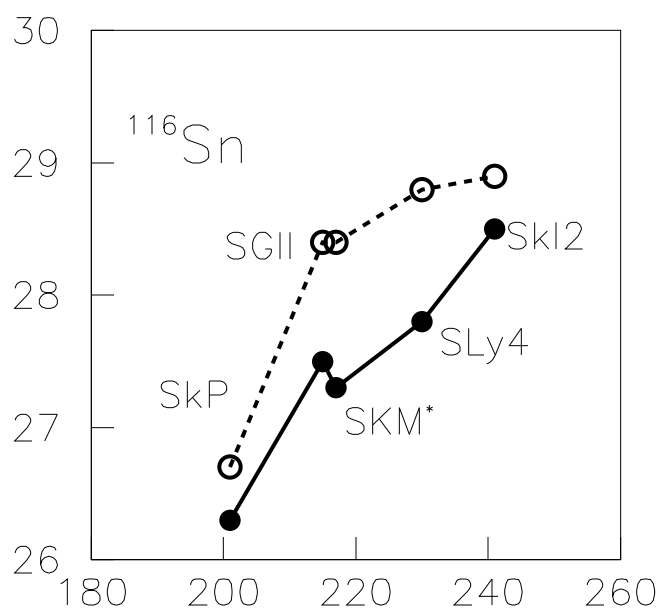
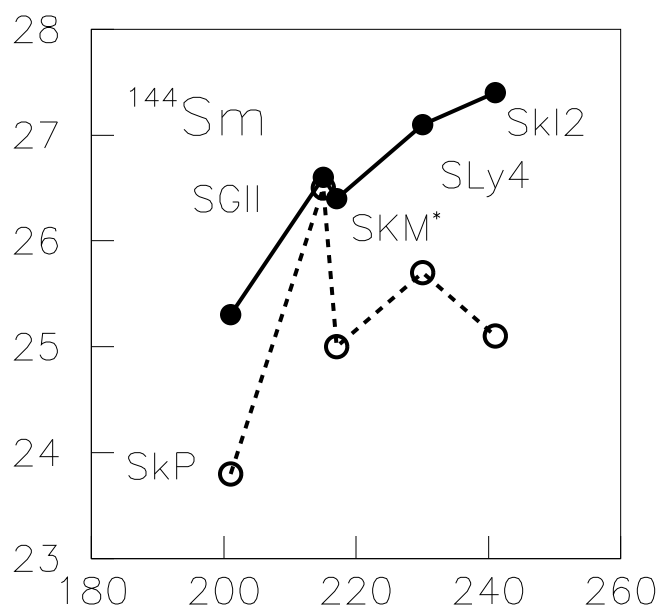
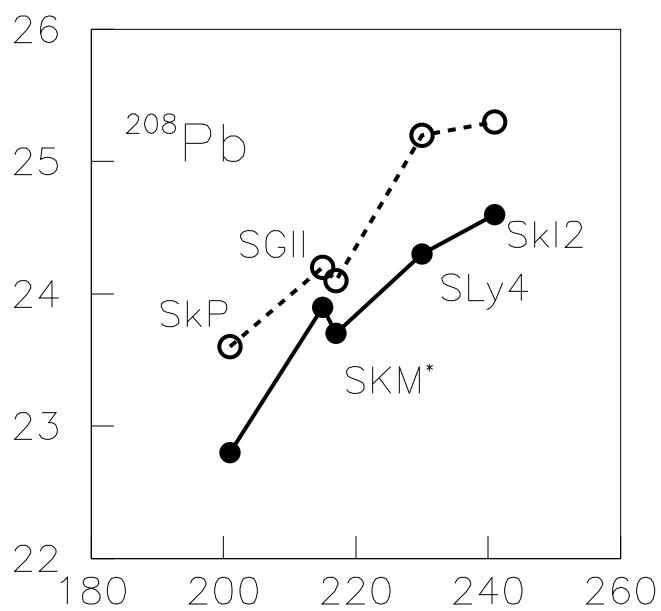
Table 2: Same as in Table 1, for the 4 nuclei calculated with SGII.

Nucleus	Range of GR region	Low-energy region		GR region		
		m_0	m_1	m_0	m_1	m_1/m_0
^{208}Pb	17-30	0.90	0.98	1.61	3.85	23.9 (24.1)
^{144}Sm	21-32	0.34	0.46	0.59	1.57	26.6 (26.5)
^{116}Sn	20-35	0.20	0.25	0.40	1.10	27.5 (28.4)
^{90}Zr	22-40	0.11	0.16	0.21	0.63	30.0 (26.7,32.5)



ISGDR Strength [fm⁶ MeV⁻¹]

Energy [MeV]



ISGDR energy E_0 [MeV]

K [MeV]